CHEMICAL ENGINEERING TRANSACTIONS
VOL. 74, 2019
A publication of AIDIC
The Italian Association of Chemical Engineering
Online at www.cetjournal.it
Guest Editors: Sauro Pierucci, Jiří Jaromír Klemeš, Laura Piazza

ISBN 978-88-95608-71-6; **ISSN** 2283-9216
DOI: 10.3303/CET1974154

Effective Strategy for Numerical Discretization In DRPSA Detailed Modeling

Ester Rossi[a], Giuseppe Storti[b], Renato Rota[a,*]

[a] Chemistry, Materials and Chemical Engineering Department "Giulio Natta", Politecnico di Milano, Via Mancinelli 7, 20131 Milan, Italy
[b]ETH Zürich, Department of Chemistry and Applied Biosciences, Vladimir-Prelog-Weg 1-5/10, HCI F 125, 8093 Zürich, Switzerland
renato.rota@polimi.it

Since high performance separations can be achieved, design and modeling of the Dual Reflux Pressure Swing Adsorption (DRPSA) process are topics of great interest. DRPSA is a cyclic process whose dynamic behavior requires an accurate description of the steep gradients of concentrations, which develop and propagate along the bed during the process. Moreover, this process is intrinsically non-stationary. Therefore, Cyclic Steady State (CSS) can be established, which requires simulating the process dynamics for a large (even undefined) number of cycles. The complexity in representing DRPSA dynamics is the reason why research efforts have been recently spent to develop numerical models detailed enough to reliably describe the separation evolution. A suitable spatial discretization of the system equations is needed in order to be sure that the results do not depend on the selected grid size. At the same time, as the number of grid points increases, the time required for the simulation increases too. Therefore, in this work, we propose a general and effective strategy to automatically select a spatial discretization, which guarantees that the simulation results are grid-independent and, at the same time, that the true CSS is reached with a minimal computational effort. To do this, we resort to approaches available in literature for Pressure Swing Adsorption processes and formulate a new strategy tailored for DRPSA. This approach has been applied together with the Finite Volume Method as numerical discretization approach, but it can be adapted to any numerical strategy.

1. Introduction

Nowadays, the growing industrial development, related to a significant usage of fossil fuel, makes the Carbon Capture and Storage (CCS) a key topic (Geng and Meng, 2018). In the CCS domain, the Pressure Swing Adsorption (PSA) process plays an important role in the separation of gas mixtures containing CO_2. As a matter of fact, PSA is a widely used technology in the gas separation framework (Stinguel and Guirardello, 2017). This process name is due to the fact that the separation is obtained through a continuous switching of the total pressure between two different values. It is a cyclic process which usually involves at least two adsorption beds working simultaneously. When considering the separation of binary gas mixtures, the traditional configurations are affected by an inherent thermodynamic limitation which allows (for a given pressure ratio) the complete separation of only one of the two components (Yoshida et al., 2003). To overcome this limit, a new PSA configuration was proposed in 1992 by Leavitt (Leavitt, 1992), the so-called DRPSA. It is based on the same idea behind PSA, but involves two refluxes which, together with a lateral feed injection, enable the process to achieve complete separation of a binary mixture (Kearns and Webley, 2006). This capability is the reason of a significant research interest in this area, especially on the modelling side (Bhatt et al., 2015; May et al., 2017). When modelling this process, the internal loops lead to strongly coupled behaviour of the adsorption beds. Moreover, DRPSA is a non-stationary process, which means that CSS conditions are established and the accurate representation of the periodical dynamic behaviour is a challenge. Two major approaches are discussed in the available modelling literature. In the first case, simplified but analytically solvable models based on the so-called *Equilibrium Theory* (Ebner and Ritter, 2004) are used. Due to the many underlying assumptions, these models are effective as conceptual design tools but may be

Paper Received: 27 June 2018; Revised: 13 December 2018; Accepted: 27 March 2019

Please cite this article as: Rossi E., Storti G., Rota R., 2019, Effective Strategy for Numerical Discretization in Drpsa Detailed Modeling, Chemical Engineering Transactions, 74, 919-924 DOI:10.3303/CET1974154

not adequate for a realistic description of the process in the general case. On the other hand, detailed models involving systems of Partial Differential Equations (PDEs) are considered in the second case, where ad-hoc numerical schemes are required for accurate numerical solutions in acceptable computational times. Therefore, the anticipated complexity of the DRPSA dynamic modelling makes the judicious selection of an effective numerical strategy a key aspect.

The aim of this work is to provide an efficient strategy to limit the computational efforts simultaneously ensuring the reliability of the results. In particular, when simulating a DRPSA process through a detailed model, the *a priori* definition of the adequate grid size for the spatial discretization is difficult. Typically, a first trial grid size is selected and, after reaching CSS, refined to investigate if the results are grid independent. It is evident that a lot of simulations are required in this case. The methodology proposed in this work permits the selection of the optimal grid size (ensuring grid-independent results along with CSS establishment) with minimum computational effort. The approach is validated using a literature DRPSA model, numerically solved by the Finite Volume Method (FVM) for the spatial discretization (Rossi et al., 2019).

2. Process description and modeling

The basic cycle of the DRPSA process involves four steps: the feed step (FE) in which the adsorption on the solid occurs; the purge step (PU) during which a bed is regenerated; the pressurization step (PR) through which a bed is brought to the highest operating pressure; a blowdown step (BD) in which the operating pressure is reduced to the lowest value. Based on the operating pressure at which the FE step is performed, high or low pressure, and on which stream is exploited to perform the switching of pressures, light or heavy product, four different process configurations are usually identified (Kearns and Webley, 2006). In this work, we consider a so-called DRPHA process, characterized by FE operated at high pressure and pressurization performed with the heavy product stream (see Figure 1 for the schematic of one half of the complete cycle).

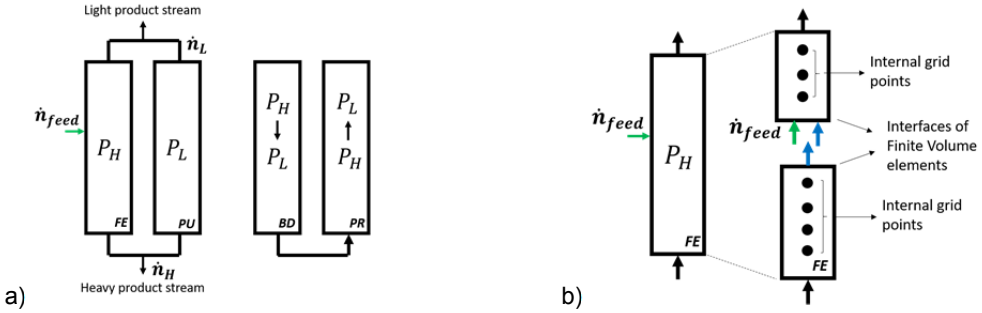

Figure 1: (a) Process scheme and (b) schematization of the lateral feed injection.

The developed model of the DRPHA process is based on the following main assumptions:

- ideal gas law;
- isothermal process;
- Linear Driving Force (LDF) approximation for mass transfer;
- Blake-Kozeny equation for pressure drops;
- negligible axial dispersion.

The resulting system of PDEs is made of Eqs(1)-(5):

$$\varepsilon_T \frac{\partial P}{\partial t} + \frac{\partial (uP)}{\partial z} + \rho_B RT \sum_{i=1}^{2} \frac{\partial q_i}{\partial t} = 0 \tag{1}$$

$$\varepsilon_T \frac{\partial (Py_i)}{\partial t} + \frac{\partial (uPy_i)}{\partial z} + RT\rho_B \frac{\partial q_i}{\partial t} = 0 \tag{2}$$

$$\frac{\partial q_i}{\partial t} = k_{LDF,i}(q_i^* - q_i) \tag{3}$$

$$\frac{\partial P}{\partial z} = -\frac{u}{\frac{150}{4}\frac{1}{r_p^2}\left(\frac{1-\varepsilon_B}{\varepsilon_B}\right)^2 \mu} \tag{4}$$

$$q_i^* = f(P, y_i). \tag{5}$$

where P is the total pressure, y_i the molar fraction of A or B, u the superficial velocity, $k_{LDF,i}$ the LDF coefficient of i, q_i the adsorbed amount of i, q_i^* the adsorbed amount of i in equilibrium conditions, R the gas constant, r_p the radius of an adsorbent particle. A complete list of all model variables is provided in Table 1. The independent variables of this system of PDEs, v_i, are lumped together into the state variable vector $V = [y_i, q_i, P, u]$. The efficient numerical solution of the resulting system of PDEs is crucial to the effective use of the model in the design and optimization of DRPSA processes. In this work, we applied a numerical strategy based on the FVM joint with a combination of Van Leer's Flux Limiters, first order upwind interpolations and Lagrange extrapolations for the spatial domain (Rossi et al. 2019).

3. Strategy for the numerical discretization

As previously mentioned, a DRPSA process is inherently non-stationary and Cyclic Steady State (CSS) conditions are of primary interest to process design. In order to evaluate the true CSS performances of the unit, the DRPSA cycle has to be simulated for a number of cycles large enough to reach this CSS. At the same time, a non-realistic solution is found if the number of computational nodes is not sufficient to guarantee grid-independent results. About the computational grid selection, univocally adopted guidelines towards the best choice are not available. Moreover, the establishment of CSS conditions can be differently defined, for example based on the repetition of the cycle-average composition of each product stream (Zhang et al., 2016), but also on the extent of closure of the material balances (Bhatt et al., 2015). To simultaneously deal with these two aspects, in this work we develop a systematic strategy for defining a grid size with an adequate number of computational nodes, i.e. leading to a reliable CSS solution. For the prediction of the CSS, we resort to a criterion developed by Effendy and co-workers in 2017 (Effendy et al., 2017) for the PSA process, here adapted to the peculiar DRPSA configuration. Then, we define a node refinement strategy, inspired to the one developed for PSA by Todd and co-workers in 2001 (Todd et al., 2001), introducing a criterion to *a priori* define the minimum number of grid points for the simulation together with an efficient criterion to stop the grid size refinement.

3.1 Strategy description

The steps of the proposed methodology are the following:

1. select the minimum number of grid points used to discretize the column length;
2. solve numerically the PDEs until a preliminary fulfillment of CSS conditions (based on a suitable indicator);
3. increase (for example, double) the number of grid points;
4. solve numerically the PDEs again until the preliminary fulfillment of CSS conditions;
5. compare the final results of the two last simulations through another indicator of grid-independence results: if the results are not grid independent, return to step 3;
6. solve numerically the PDEs until the complete fulfillment of CSS conditions based on the corresponding indicator.

To implement such a procedure, the minimum number of grid points as well as the CSS and grid-independence indicators have to be defined, as discussed in the following.

Since the selected numerical method has a maximum order of interpolation equal to 3 (Rossi et al., 2019), in order to use at least one time the higher interpolation order of the numerical scheme for each semi-column, a minimum of 6 nodes is required. Moreover, a further constraint to the minimum number of grid points arises from the discrete locations allowed for the feed injection position. In fact, the lateral feed injection represents a discontinuity in the adsorption bed, which can be represented as two semi-columns in series (see Figure 1b). Let us consider the limit case in which only two computational nodes are used to model the whole adsorption bed, as in the computational domain represented in Figure 2. When the lateral feed injection is in $\bar{z}_{feed} = 0.3$ (which corresponds to 30% of the column length, being $\bar{z}_{feed} = z/L$), since it should be located at the nearest interface of a finite volume element, its discretized location will be at $I2$. However, if $\bar{z}_{feed} = 0.2$ (which corresponds to 20% of the column length), the feed inlet should be located at $I1$. This means that the feed inlet moves to the column end, a poor approximation of its actual intermediate position. In other words, the first 25% of the column length (and analogously the last 25%) cannot be represented as lateral feed position when using two grid points (red areas in Figure 2). Of course, this limitation vanishes by increasing the number of grid points and the red areas reduce to 5% of the length from top and bottom of the column when using 10 finite volumes. Since the length of such excluded portions of the columns is negligible ($\bar{z}_{feed}$ values smaller than 0.05 or larger than 0.95 are impractical, cf. Bhatt et al., 2013), 11 computational nodes (N) can be assumed as the minimum number of grid points.

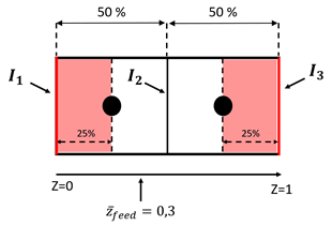

Figure 2: Example of computational grid with $N = 2$.

As an indicator for CSS establishment, the norm error between the current state of the system, represented by the values of the state variables computed at the current cycle, and that at CSS has been used (Effendy et al., 2017). CSS conditions are therefore established when $\Delta e_n/\Delta e_0 < \alpha$, where α is a defined tolerance and Δe_n represents the variation of the bed conditions from cycle n to cycle $n+1$, defined as:

$$\Delta e_n = e_{n+1} - e_n = \frac{1}{lenght(V)} \sum_{v \in V} \int_0^1 |v_{n+1} - v_n| dz \tag{6}$$

being Δe_0 the variation of the bed conditions from the initial conditions to the end of the first cycle. A value of α equal to $5 \cdot 10^{-2}$ has been set as "rough" indication of CSS reaching.
According to the procedure outlined above, once the CSS is reached with the minimum number of nodes, a finer grid with $N_1 = 2 \cdot N_0$ is set and a new simulation is carried out using the CSS solution obtained with N_0 nodes as initial condition. The new simulation is run until the CSS indicator is smaller than the prescribed value $\alpha = 5 \cdot 10^{-2}$ and the procedure is iterated. The sequence is interrupted when two successive simulations give very similar solutions, as quantified by the grid-independence indicator. In this work, such indicator was the percentage error ξ_N, defined as:

$$\xi_{N_x} = \left(\sum_{j=1}^{N_0} \frac{\left| \hat{y}_{j,\frac{N_x}{2}} - \hat{y}_{j,N_x} \right|}{y_{j,N_0}} \right) \cdot 100 \tag{7}$$

where the profiles of the molar fraction of species *A* (the most adsorbable component) at the end of the FE step at CSS have been used. In order to compare the molar fraction profiles evaluated at different number of grid points, N_x, the profile $\hat{y}_{N_x} = [\hat{y}_{1,N_x}, \dots, \hat{y}_{N_0,N_x}]$ is built just interpolating that obtained with N_x computational nodes in the smaller domain defined by the minimum number of nodes N_0. When ξ_{N_x} is smaller than a threshold value, say 20%, the results are considered grid-independent. Finally, the last simulation is repeated using the much more demanding value of the CSS indicator $\alpha = 5 \cdot 10^{-4}$.

3.2 Case study

The efficiency of the strategy developed in this work has been assessed through a case study, whose main input data are summarized in Table 1.

Table 1: Case-study process parameters

Symbol	Description	Value	Symbol	Description	Value
ε_B	Bed void fraction	0.31	μ	Viscosity	$1.8 \cdot 10^{-5}\ Pa \cdot s$
ε_T	Total void fraction	0.76	t_{feed}	Duration of the FE	$180\ s$
P_L	Low pressure	$1\ Pa$	t_{press}	Duration of the PR	$400\ s$
P_H	High pressure	$2\ Pa$	$\dot{n}_L$	Reflux flowrate	$2.25 \cdot 10^{-5} mol/s$
$y_{A,feed}$	Molar fraction of A fed	0.79	$\dot{n}_{feed}$	Feed flowrate	$1.83 \cdot 10^{-5} mol/s$
T	Temperature	$303\ K$	$\dot{n}_H$	Heavy product flowrate	$1.44 \cdot 10^{-5} mol/s$
ρ_s	Density of the solid	$3{,}310 kg/m^3$	$\bar{z}_{feed}$	Lateral feed injection position (dimensionless, being $\bar{z} = z/L$)	0.86
ρ_B	Density of the bed	$795\ kg/m^3$	H_A	Linear adsorption isotherm coefficient, component A	$2.3 \cdot 10^{-6} mol/kgPa$
L	Length of the bed	$1\ m$	H_B	Linear adsorption isotherm coefficient, component B	$1 \cdot 10^{-6} mol/kgPa$
D	Diameter of the bed	$0.03\ m$			

The selected operating conditions correspond to the complete separation of the components A and B of a binary mixture when the so-called *Equilibrium Theory* applies (Bhatt et al., 2013). In order to fulfill the assumptions behind the equilibrium theory, linear equilibrium isotherms $q_i^* = H_i \cdot P \cdot y_i$ have been selected (Eq. (5)). Moreover, the values of mass transport coefficients in Eq.(4) and particle radius are set large enough to make negligible the mass transfer resistances and the pressure drops. Notice that, a complete separation case is selected since its numerical simulation is particularly demanding because of the steep profiles typically established and, consequently, to challenge the efficacy of the proposed strategy.

4. Results and discussion

Starting from an initial value of the grid points $N_0 = 11$, a final value of $N = 176$ has been determined and applied for the final simulation using the minimum value of the CSS indicator $\alpha = 5 \cdot 10^{-4}$. The main results of the aforementioned case study are summarized in Figures 3 to 5.

Figure 3: Purities of both A and B obtained with $\alpha = 5 \cdot 10^{-4}$ as a function of Nx.

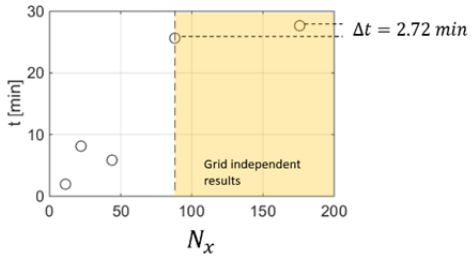

Figure 4: Overall computational time t for the strategy proposed as a function of Nx.

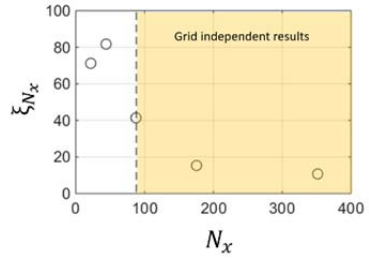

Figure 5: ξ_{N_x} as a function of Nx.

The predicted purities of both species A and B computed using the proposed methodology at CSS with the smallest value $\alpha = 5 \cdot 10^{-4}$ are shown in Figure 3. The simulated results are not accurate enough when the grid-independence of the results is not properly verified, as evident from the latter figure. It shows as for Nx values lower than 88 both the purities of light and heavy product are strongly underestimated, even if CSS conditions are satisfied.

Differently, the results obtained with more than 88 grid points are not only consistent (thus corresponding to complete separation), but also grid-independent. Quite interestingly, the overall computational time required to simulate CSS conditions with accuracy (that is, carrying out the simulation with a given number of grid points until a value of the CSS indicator lower than $\alpha = 5 \cdot 10^{-4}$) as a function of N_x becomes almost unaffected by

the number of grid points once grid-independent conditions are established (see Figure 4). This means that an overestimation of the minimum value of N_x probably carried out by doubling this value at each iteration step is not affecting the computation effort at significant extent.
Moreover, focusing on Figure 5, the trend of the grid independence indicator ξ_{N_x} over Nx is shown. We can consider as indicative the ξ_{N_x} monitoring, since when the grid independence is reached (i.e., for $N > 88$) its value becomes almost constant and lower than about 20%.
In conclusion, the strategy presented in this work suggests a way to define a suitable spatial discretization for any DRPSA process simulation and does not require any knowledge on the dynamic behavior of the process investigated.

References

Bhatt, T. S., Storti, G., Rota, R., 2013. Optimal design of dual-reflux pressure swing adsorption units via equilibrium theory, Chemical Engineering Science 102, 42-55.
Bhatt, T. S., Storti, G., Rota, R., 2015. Detailed simulation of dual-reflux pressure swing adsorption process, Chemical Engineering Science 122, 34-52.
Ebner, A. D., Ritter, J. A., 2002. Equilibrium theory analysis of rectifying PSA for heavy component production, AIChE Journal 48(8), 1679-1691.
Effendy, S., Farooq, S., Ruthven, D. M., 2017. A rigorous criterion for approach to cyclic steady-state in PSA simulations, Chemical Engineering Science 160, 313-320.
Geng S., Meng W., 2018, Chemical absorption and mass transfer of greenhouse gas carbon dioxide, Chemical Engineering Transactions, 71, 1-6.
Kearns, D. T., Webley, P. A., 2006. Modelling and evaluation of dual-reflux pressure swing adsorption cycles: Part I. Mathematical models, Chemical Engineering Science 61(22), 7223-7233.
Leavitt, F. W. 1992. Duplex Adsorption process, US Patent 5,085,674.
May, E. F., Zhang, Y., Saleman, T. L., Xiao, G., Li, G. K., Young, B. R., 2017. Demonstration and optimisation of the four Dual-Reflux Pressure Swing Adsorption configurations. Separation and Purification Technology, 177, 161-175.
Rossi, E., Paloni, M., Storti, G., Rota, R., 2019. Modeling Dual Reflux-Pressure Swing Adsorption processes: numerical solution based on the Finite Volume Method, Chemical Engineering Science 203, 173-185.
Stinguel, L., Guirardello, R., 2017. Evaluation of a Simplified Model of Adsorption used to Separate Ethanol-Water, Chemical Engineering Transactions, 57, 1057-1062.
Todd, R. S., He, J., Webley, P. A., Beh, C., Wilson, S., Lloyd, M. A., 2001. Fast finite-volume method for PSA/VSA cycle simulation - Experimental validation, Industrial and Engineering Chemistry Research 40(14), 3217-3224.
Yoshida, M.; Ritter, J. A.; Kodama, A.; Goto, M.; Hirose, T., 2003. Enriching reflux and parallel equalization PSA process for concentrating trace components in air, Industrial and Engineering Chemistry Research, 8, 1795-1803.
Zhang, Y., Saleman, T. L. H., Li, G. K., Xiao, G., Young, B. R., May, E. F., 2016. Non-isothermal numerical simulations of dual reflux pressure swing adsorption cycles for separating N2 + CH4, Chemical Engineering Journal 292, 366-381.